Phys. Status Solidi B **251**, No. 12, 2581–2586 (2014) / **DOI** 10.1002/pssb.201451168

physica status solidi b
www.pss-b.com
basic solid state physics

Enhanced electrical and mechanical properties of nanographite electrodes for supercapacitors by addition of nanofibrillated cellulose

Britta Andres*[,1], Sven Forsberg[1], Christina Dahlström[2], Nicklas Blomquist[1], and Håkan Olin[1]

[1] Department of Natural Sciences, Mid Sweden University, SE-851 70 Sundsvall, Sweden
[2] Department of Chemical Engineering, Mid Sweden University, SE-851 70 Sundsvall, Sweden

Received 15 April 2014, revised 15 October 2014, accepted 16 October 2014
Published online 18 November 2014

Keywords graphene, graphite, nanofibrillated cellulose, nanographite, paper, supercapacitor

* Corresponding author: e-mail britta.andres@miun.se, Phone: +46-60-148671, Fax: +46-60-148820

Graphene and porous carbon materials are widely used as electrodes in supercapacitors. In order to form mechanically stable electrodes, binders can be added to the conducting electrode material. However, most binders degrade the electrical performance of the electrodes. Here we show that by using nanofibrillated cellulose (NFC) as a binder the electrical properties, such as capacitance, were enhanced. The highest capacitance was measured at an NFC content of approximately 10 % in ratio to the total amount of active material. The NFC improved the ion transport in the electrodes. Thus, electrodes made of a mixture of nanographite and NFC achieved larger capacitances in supercapacitors than electrodes with nanographite only. In addition to electrical properties, NFC enhanced the mechanical stability and wet strength of the electrodes significantly. Furthermore, NFC stabilized the aqueous nanographite dispersions, which improved the processability. Galvanostatic cycling was performed and an initial transient behaviour of the supercapacitors during the first cycles was observed. However, stabilized supercapacitors showed efficiencies of 98–100%.

1 Introduction A supercapacitor stores energy by separating charges at the interface between the electrodes and the electrolyte [1]. An electric double-layer is formed, and positive ions accumulate on the negative electrode surface and negative ions on the positive electrode. The capacitance of a supercapacitor and, thus, its energy storage capacity is proportional to the double-layer area. Therefore, electrodes with a high specific surface area are desired [1]. Research on electrode materials for supercapacitors has generated a number of advanced active materials [2, 3]. Porous carbon materials are the first choice for most supercapacitor electrodes. Different grades of activated carbon [2, 4], carbon nanotubes [2, 4, 5], graphene [6] and other conductive materials [2, 4] show a good electrode performance. However, most advanced materials are costly and not suitable for an inexpensive large-scale production. Therefore, we are focussing on inexpensive materials such as graphite. We produced exfoliated graphite, here called nanographite, which is a mixture of graphene, multi-layer graphene and graphite. Nanographite was prepared by mechanical exfoliation of a graphite-water dispersion in a high-pressure homogenizer. The mechanical and electrical properties of the nanographite were compared to a commercially available graphite powder, here called battery-graphite. The battery-graphite is usually used to increase the electrical conductivity in battery electrodes, but can be used for the same purpose in electrodes for supercapacitors.

Further requirements for the electrode material are a low electrical resistance and a large surface area to achieve high capacitances in supercapacitors. A high mechanical stability and a high wet strength of the electrodes are desired because the electrodes are subjected to strong mechanical forces during production, supercapacitor assembly and the operation in liquid electrolytes. Weak electrodes or binder-free electrodes will break even at low loads. Furthermore, a good processability of the electrode material is crucial to facilitate a large-scale production using roll-to-roll techniques [7]. Mechanical stability and wet strength can be obtained

by adding binders. To maintain good electrical properties of the electrode material, binders should not decrease the electrical conductivity of the electrodes. Since we are targeting inexpensive, environmentally friendly, paper-based supercapacitors [8], we were using nanofibrillated cellulose (NFC) as an additive to enhance the electrode stability. NFC, also called nanocellulose or microfibrillated cellulose, is a wood-based nanomaterial made of cellulose fibrils. It can be produced by disintegration of cellulose fibres, mostly wood-based fibres, in a homogenizer [9]. The amorphous nanofibrils have a length of up to several μm and a width of 5–60 nm [10]. NFC can be used as separator and binder in electrodes [11] for Li-ion batteries [12–14] and the use of cellulose-carbon nanotube composites in supercapacitors has also been reported [15]. However, the use of NFC–graphite composites in supercapacitors has not been studied. Therefore, we tested the electrical performance of nanographite–NFC electrodes in supercapacitors. We investigated if NFC influences the electrode structure and whether it can enhance the supercapacitor's capacitance.

2 Materials and method To prepare the nanographite, thermally expanded graphite (SO# 5-44-04) from Superior Graphite was dispersed in water. A dispersion with a graphite concentration of 20 g/l was mechanically exfoliated in a high-pressure homogenizer (GEA Niro Soavi, ARIETE, Model: NS2006H). The homogenizer was operated at approximately 400 bar for 2 hours. The dispersion passed the shear zone of the homogenizer 21 times. After dewatering the homogenized graphite, the resulting graphite paste had a solids content of 13.4 %. It contained a mixture of graphene, multi-layer graphene and larger graphite particles. Furthermore, BET measurements were performed using a Micromeritics modell 2300 BET. The nanographite showed a specific surface area of 19.2 m^2/g. To confirm the presence of single-layer and multi-layer graphene, transmission electron microscope (TEM) and atomic force microscope (AFM) images were taken using a JEOL-2000FX and a Nanoscope IIIa. The images can be seen in Fig. 1. Both single-layer graphene, which has a theoretical thickness of 0.335 nm, and multi-layer graphene sheets could be located.

Battery-graphite (ABG 2025, SO# 5-42-25) from Superior Graphite was used as received.

TEMPO-oxidized NFC was prepared according to the method described in [16]. By using 5 mmol sodium hypochlorite (NaClO) instead of 1 mmol NaClO, NFC with a higher charge density was produced. Conductometric titration showed a charge density of 1.5 mmol/g. An NFC gel with a concentration of 20 g/l was obtained. The NFC gel was further diluted with deionized water to give a concentration of 4 g/l. NFC was employed as a binder for the electrodes.

Greaseproof paper (untreated, grammage: 45 g/m^2) from Nordic Paper was used as separator in the supercapacitors. Sodium sulfate (Na_2SO_4) from Sigma Aldrich dissolved in deionized water served as the electrolyte. A concentration of 1 mol/l was used.

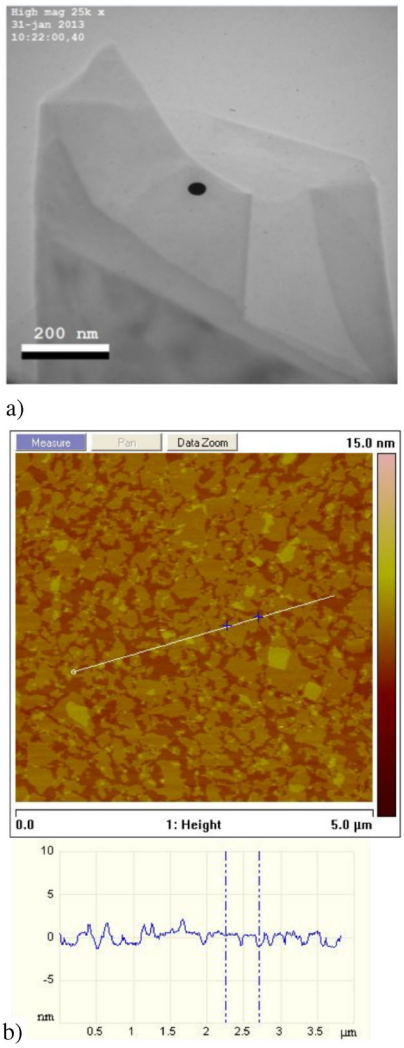

Figure 1 (a) TEM image and (b) AFM image and height profile of nanographite flakes.

2.1 Preparation and testing of electrodes Electrode films with mixtures of NFC and nanographite (Series A), and NFC and battery-graphite (Series B) were prepared. All films contained 0.42 g dried active material, i. e. nanographite or battery-graphite. The amount of NFC varied from 0 % (sample A0 and B0) to 20 % (sample A20 and B20). The amount of NFC is stated in % of the total graphite mass.

First the carbon was mixed with NFC and approximately 20–30 ml deionized water. The dispersions were mixed with an IKA T25 digital Ultra Turrax at 12000 rpm for 10 minutes. Afterwards, each dispersion was filtrated with 200 ml deionized water on a Millipore Durapore Membrane Filter (filter type: 0.22 μm GV). The obtained graphite films were dried at room temperature.

The thickness of the dried electrode films was measured using a Mahr Millitast 1083. The median of five measurements was calculated.

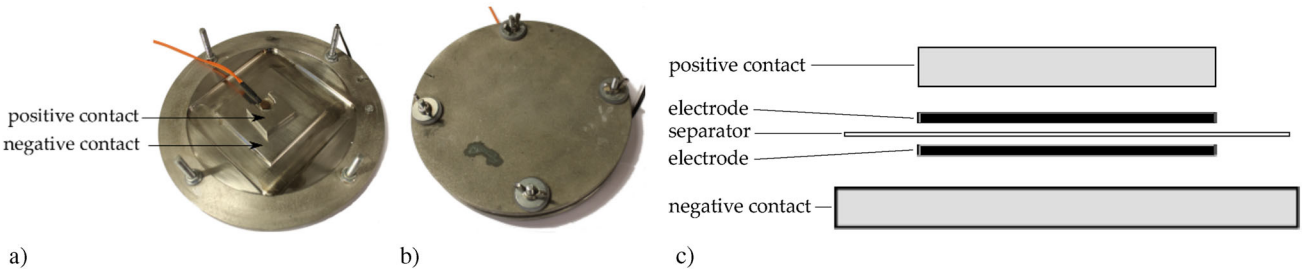

Figure 2 Test-setup for supercapacitor testing. (a) Test cell for single- and multi-cell supercapacitor testing. (b) Sealed test-cell. (c) Schematic of a supercapacitor in the test cell.

Sheet-resistance measurements were performed in a conditioning chamber at 23 °C and a relative humidity of 50 %. The samples were stored in the chamber for 30 minutes prior to the measurements to ensure constant conditions for all samples. A Hewlett Packard 3457A Multimeter was used to measure the sheet-resistance. It was set to four-point probe mode. The median of five measurements was calculated.

In addition, we examined the internal structure of the electrodes by using a scanning electron microscope (SEM) on the cross section of the electrode films. High quality cross sections were prepared with a Hitachi IM4000 Ion Milling System (Hitachi High-Technologies Corporation, Japan). Afterwards the samples were sputtered with carbon to obtain an electrically conducting surface. The cross sections were investigated using a LEO 1450EP scanning electron microscope.

2.2 Preparation and testing of supercapacitors

Figure 2a shows the setup that was used to test the supercapacitors. The stainless steel construction is equipped with an adjustable top casing to vary the pressure load on the supercapacitor, see Fig. 2b. Furthermore, the setup is sealed by a rubber ring to prevent evaporation of the electrolyte.

To test a supercapacitor, we build a stack as illustrated in Fig. 2c. One electrode is placed on each side of the paper separator. The electrodes are 2.9 cm×2.9 cm, resulting in an area of 8.4 cm^2 each, while the separator is slightly larger than the electrodes (approximately 5 cm×5 cm) in order to avoid short circuits at the edges. The separator was soaked with electrolyte prior to the assembly. Before contacting the electrodes to the stainless steel contacts we wet the electrodes with electrolyte. Sodium sulfate (1 mol/l) was used as the electrolyte due to its almost neutral, slightly acidic pH.

Constant current charge-discharge cycles were plotted using a LabVIEW-based PXI system. The collected data was analysed according to the method described by Stoller and Ruoff [17]. The capacitance C of the supercapacitors was calculated from the discharge curves by

$$C = I \cdot \frac{\mathrm{d}t}{\mathrm{d}V}, \tag{1}$$

where the variable I is the discharge current, $\mathrm{d}t$ the discharge time and $\mathrm{d}V$ the voltage difference. The discharge current I was chosen to give a current density of 0.1 A/g, which refers to the current per mass of one electrode. Previous measurements showed that the curve shape of the first charge and discharge cycles differs from the subsequent cycles. Thus, the capacitance of the 4000th cycle was calculated to compare the performance of the supercapacitors.

The efficiency η of the supercapacitor was calculated by dividing the discharge time by the charge time.

3 Results and Discussion

3.1 Mechanical stability and wet strength The electrode films were examined visually before and during the supercapacitor assembly. Figure 3 compares electrode films made from battery-graphite in terms of mechanical stability in dry and wet conditions. Figure 3a and 3b show two electrode films that were subjected to a light load. Sample B0 (Fig. 3a) does not contain NFC and thus has a poor mechanical stability. The sample cracks immediately if touched. In contrast, sample B10 (Fig. 3b) contains 10 % NFC and shows a reasonable mechanical stability. The films containing NFC can be cut easily and maintain their shape even after the operation in a supercapacitor. Electrodes with less than 5 % NFC collapse during supercapacitor assembly or during supercapacitor operation. The same applies for the wet strength of the films. Samples with at least 5 % NFC maintain their stability when operated in electrolyte, see Fig. 3d. Electrodes without NFC degrade when soaked in electrolyte. They soften, and loose particles were floating in the electrolyte, see Fig. 3c. The observations described in this paragraph and displayed in Fig. 3 were similar for the nanographite films.

Graphite–NFC films even show a good bendability. Both dry and wet films containing more than 10 % NFC can be bent, see Fig. 4. However, films break when folded.

In summary, we can report that NFC can be used to improve the mechanical strength of the electrodes, which is in agreement with the results discussed in [13, 14]. As a result, the processability of graphite electrodes was enhanced.

In addition to an improved mechanical stability, we observed that the stability of aqueous nanographite dispersions can be enhanced by adding NFC. Figure 5 compares two nanographite dispersions, one without NFC (left vial) and one with 10 % NFC (right vial). The photo was taken 10 minutes after the materials were mixed. The nanographite without NFC formed aggregates within just a few minutes.

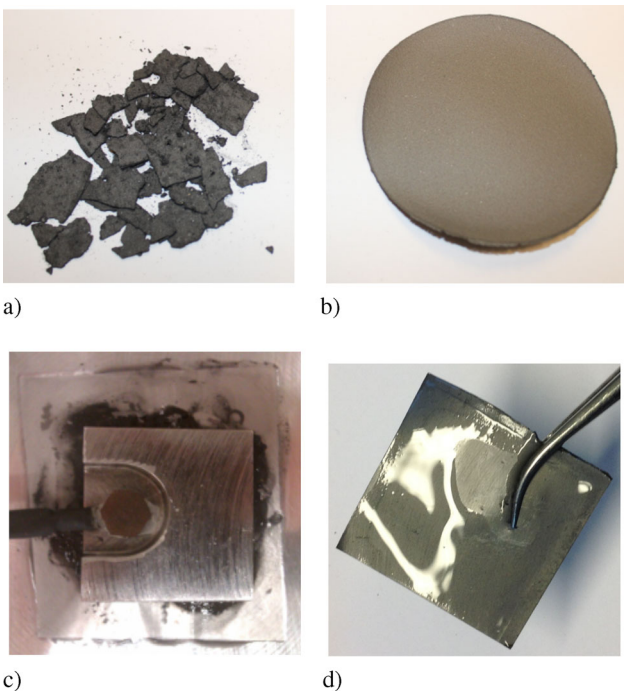

Figure 3 Mechanical stability and wet strength of battery-graphite films. (a) Battery-graphite film without NFC (sample B0) after light load. (b) Battery-graphite film with 10 % NFC (sample B10) after light load. (c) Battery-graphite film without NFC (sample B0) after operation in a SC. (d) Battery-graphite film with 10 % NFC (sample B10) after operation in a SC.

Most nanographite sedimented, and some aggregates floated on top of the dispersion. The dispersion with NFC, however, did not sediment directly. We could not observe any larger agglomerates during the first hours, but after approximately four hours small agglomerates could be found at the bottom of the vial.

Figure 4 Bent nanographite–NFC film after operation in a SC.

Figure 5 Stability of nanographite dispersions without NFC (left vial) and with 10 % NFC (right vial).

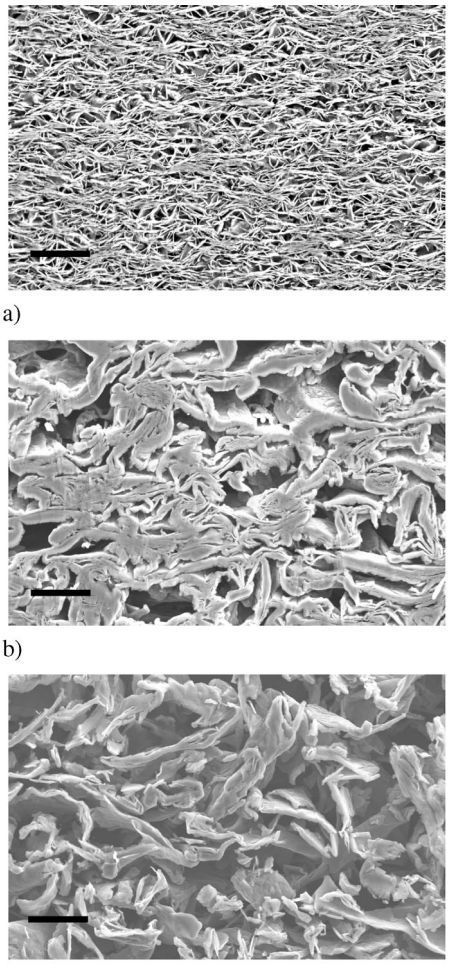

Figure 6 Cross section SEM images of nanographite and battery-graphite electrodes with and without additional 10 % NFC. The black bar is 20 μm. (a) Nanographite electrode with 10 % NFC (sample A10). (b) Battery-graphite electrode with 10 % NFC (sample B10). (c) Battery-graphite electrode without NFC (sample B0).

3.2 Electrode structure In order to obtain information about the internal structure of the graphite materials and a possible impact of NFC on the electrode structure, we compared SEM images of the electrodes' cross sections. Figure 6a and 6b show the internal structure of the two different graphite materials with additional 10 % NFC. One can clearly see a structural difference between the nanographite and the battery-graphite. The nanographite formed a denser and more uniform structure than the battery-graphite. The latter is composed of thicker and larger particle structures.

A comparison of nanographite electrodes with 10 % NFC and without any additional NFC did not reveal any change of the internal electrode structure. Both SEM images showed a similar uniform structure. However, a SEM with a higher resolution might reveal some structural difference between the pure nanographite and the nanographite–NFC composite. In contrast, a significant change in structure was seen for the battery-graphite samples, see Fig. 6b and 6c.

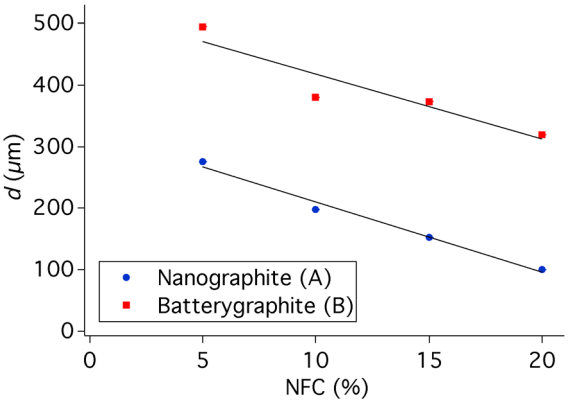

Figure 7 Thickness d of electrode films with 5–20 % NFC and nanographite or battery-graphite as active material. The black lines represent trend lines.

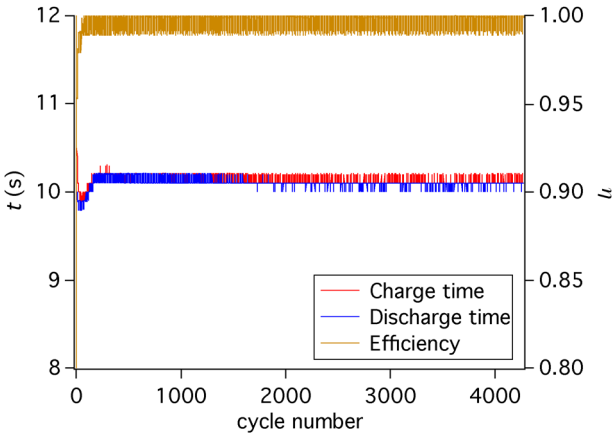

Figure 9 Charge and discharge times and efficiency for each cycle of a typically 24 hours constant current measurement.

Electrodes containing NFC showed a more dense structure than pure battery-graphite electrodes. In order to evaluate whether the structural change influences the electrode performance in supercapacitors, measurements of the porosity and the pore size distribution should be compared with capacitance measurements.

Measurements of the electrode thickness confirm that the addition of NFC influences the electrode structure. Figure 7 shows that the electrode thickness decreases with increasing NFC content. This effect was observed for both types of graphite.

3.3 Electrical properties Sheet-resistance was measured on nanographite and battery-graphite electrode films with varying NFC contents. As visualized in Fig. 8, films with nanographite show a lower sheet-resistance than battery-graphite films. For both types of graphite films the sheet-resistance increases with increasing NFC content since NFC is an electrical isolator. However, electrodes with a sheet-resistance of just a few Ω/sq are well suited for operation in supercapacitors. So far, no studies on the influence of NFC on sheet-resistance of electrodes have been reported.

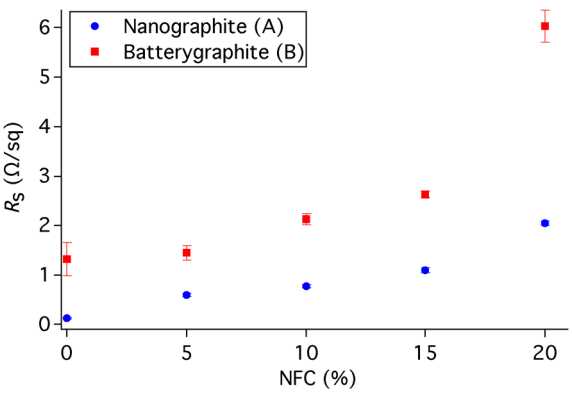

Figure 8 Sheet-resistance R_s of electrode films with 0–20 % NFC and nanographite or battery-graphite as active material.

Figure 9 shows the charge and discharge time of each cycle of a typical 24 hours constant current measurement. At the beginning of the measurement we observed an initial transient behaviour of the supercapacitor, which resulted in some longer charge and discharge times at the beginning followed by shorter times. After these initial formation cycles, however, the supercapacitor stabilized. From the charge and discharge times we calculated the efficiency of each cycle. All supercapacitors showed efficiencies between 98 and 100 %.

To determine the optimal NFC content for nanographite electrodes in terms of electrical performance in a supercapacitor, we calculated the capacitance of the 4000th cycle of each supercapacitor. The results were plotted against the NFC content, see Fig. 10. The highest capacitance can be achieved for a mixture of battery-graphite with additional 10 % NFC. Also for the supercapacitors with nanographite the highest capacitance was obtained with 10 % NFC. The amount of NFC had a less pronounced influence on the capacitance of nanographite electrodes than on battery-graphite samples.

The comparison of the SEM images of battery-graphite electrodes showed that the addition of NFC changed the

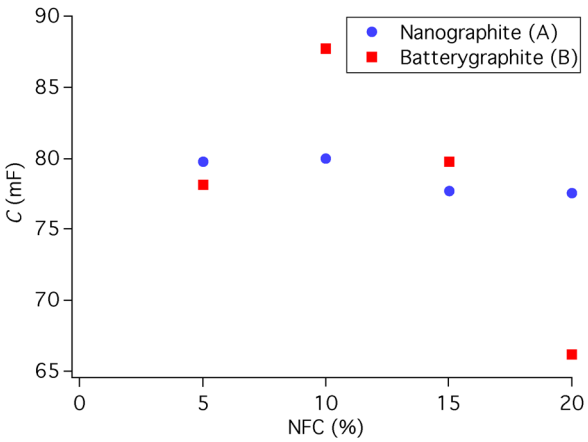

Figure 10 Capacitance of supercapacitors with graphite–NFC electrodes.

internal electrode structure. We suppose that it might have increased the electrode's surface area and thus increased the supercapacitor's capacitance. The structural change might also result in a modified pore size distribution, which can lead to a higher capacitance according to [18–20].

Another explanation for the increased capacitance is that NFC improved the ion transport in the electrodes. The NFC structure functioned as an electrolyte reservoir and provided a network of diffusion channels in the electrodes [21]. These channels improved the transport of ions in the electrode pores, which extended the internal electrode area accessible by the ions. This led to a larger electric double-layer and an improved capacitance.

Further research should be conducted on the interactions of NFC with graphite, and on the influence of NFC on the formation of an electric double-layer at the interface between the electrolyte and the NFC–graphite composite. In addition, we will improve the homogenization process to enhance the graphite quality. Since both NFC and nanographite can be produced in a high-pressure homogenizer, a combined production of the composite will be tested.

4 Conclusion In this study NFC was successfully used as a binder in nanographite and battery-graphite electrodes for supercapacitors. It improved both the brittleness and strength of the electrodes in dry and wet conditions. NFC prevented crack formation and collapse of the graphite electrodes during operation in electrolyte. Furthermore, it improved the stability of the graphite dispersions which, together with an enhanced mechanical stability, improved the processability of the electrode materials.

An addition of 10 % NFC increased the capacitance of the supercapacitors but slightly increased the sheet-resistance of the electrodes. Nanographite–NFC composites showed a low sheet-resistance preferable for use as supercapacitor electrodes. If the addition of NFC improves the capacitance, a slight increase in sheet-resistance is acceptable. Both the capacitance measurements and SEM images showed that the addition of NFC had no or only a slight impact on the structure and performance of nanographite electrodes. In contrast, a significant change in electrode structure and a distinct increase in capacitance were observed for battery-graphite electrodes.

Acknowledgements We gratefully thank Professor Lars Wågberg and Erdem Karabulut at KTH Royal Institute of Technology for their assistance and supply of NFC. We also thank Magnus Hummelgård at Mid Sweden University for programming the LabVIEW code for the potentiostat.

For the financial support we would like to thank the Swedish Energy Agency, the County Administrative Board of Västernorrland, the EU European Regional Development Fund, Bo Rydin Foundation, STT Emtec, Superior Graphite, Nordic Paper and SCA.

References

[1] T. Pandolfo, V. Ruiz, S. Sivakkumar, and J. Nerkar, in: Supercapacitors, edited by F. Béguin and E. Frąckowiak, Materials for sustainable energy and development (Wiley-VCH, Weinheim, 2013), chap. 2.
[2] P. Simon, P.-L. Taberna, and F. Béguin, in: Supercapacitors, edited by F. Béguin and E. Frąckowiak, Materials for sustainable energy and development (Wiley-VCH Verlag, Weinheim, 2013), chap. 4.
[3] M. Inagaki, in: Carbons for electrochemical energy storage and conversion systems, edited by F. Béguin and E. Frąckowiak (CRC Press, Taylor& Francis Group, Boca Raton, 2010), chap. 2.
[4] A. Yu, V. Chabot, and J. Zhang, Electrochemical supercapacitors for energy storage and delivery (CRC Press, Taylor& Francis Group, Boca Raton, 2013), pp. 151–166.
[5] K. H. An, W. S. Kim, Y. S. Park, J.-M. Moon, D. J. Bae, S. C. Lim, Y. S. Lee, and Y. H. Lee, Adv. Funct. Mater. **11**, 387 (2001).
[6] M. D. Stoller, S. Park, Y. Zhu, J. An, and R. S. Ruoff, Nano Lett. **8**, 3498 (2008).
[7] A. Giessmann, Coating Substrates and Textiles (Springer, Berlin, 2012).
[8] B. Andres, S. Forsberg, A. P. Vilches, R. Zhang, H. Andersson, M. Hummelgård, J. Bäckström, and H. Olin, Nord. Pulp Pap. Res. J. **27**, 481 (2012).
[9] M. Pääkkö, M. Ankerfors, H. Kosonen, A. Nykänen, S. Ahola, M. Österberg, J. Ruokolainen, J. Laine, P. T. Larsson, O. Ikkala, and T. Lindström, Biomacromolecules **8**, 1934 (2007).
[10] D. Klemm, F. Kramer, S. Moritz, T. Lindström, M. Ankerfors, D. Gray, and A. Dorris, Angew. Chem. Int. Ed. **50**, 5438 (2011).
[11] G. Zheng, Y. Cui, E. Karabulut, L. Wågberg, H. Zhu, and L. Hu, MRS Bull. **38**, 320 (2013).
[12] L. Jabbour, C. Gerbaldi, D. Chaussy, E. Zeno, S. Bodoardo, and D. Beneventi, J. Mater. Chem. **20**, 7344 (2010).
[13] S. Leijonmarck, A. Cornell, G. Lindbergh, and L. Wågberg, J. Mater. Chem. A **1**, 4671 (2013).
[14] S. Leijonmarck, A. Cornell, G. Lindbergh, and L. Wågberg, Nano Energy **2**, 794 (2013).
[15] V. L. Pushparaj, M. M. Shaijumon, A. Kumar, S. Murugesan, L. Ci, R. Vajtai, R. J. Linhardt, O. Nalamasu, and P. M. Ajayan, Proc. Natl. Acad. Sci. USA **104**, 13574 (2007).
[16] T. Saito, M. Hirota, N. Tamura, S. Kimura, H. Fukuzumi, L. Heux, and A. Isogai, Biomacromolecules **10**, 1992 (2009).
[17] M. D. Stoller, and R. S. Ruoff, Energy Environ. Sci. **3**, 1294 (2010).
[18] J. Chmiola, G. Yushin, Y. Gogotsi, C. Portet, P. Simon, and P. L. Taberna, Science **313**, 1760 (2006).
[19] J. Chmiola, C. Largeot, P.-L. Taberna, P. Simon, and Y. Gogotsi, Angew. Chem. Int. Ed. **47**, 3392 (2008).
[20] C. Largeot, C. Portet, J. Chmiola, P.-L. Taberna, Y Gogotsi, and P. Simon, J. Am. Chem. Soc. **130**, 2730 (2008).
[21] Z. Gui, H. Zhu, E. Gillette, X. Han, G. W. Rubloff, L. Hu, and S. B. Lee, ACS Nano **7**, 6037 (2013).

